Am J Physiol Cell Physiol 304: C458–C466, 2013.
First published January 2, 2013; doi:10.1152/ajpcell.00342.2012.

Intracellular two-phase Ca^{2+} release and apoptosis controlled by TRP-ML1 channel activity in coronary arterial myocytes

Ming Xu,[1] Xiaoxue Li,[1] Scott W. Walsh,[2] Yang Zhang,[1] Justine M. Abais,[1] Krishna M. Boini,[1] and Pin-Lan Li[1]

[1]*Department of Pharmacology and Toxicology, Medical College of Virginia Campus, Virginia Commonwealth University, Richmond, Virginia; and* [2]*Department of Obstetrics and Gynecology, Medical College of Virginia Campus, Virginia Commonwealth University, Richmond, Virginia*

Submitted 24 October 2012; accepted in final form 2 January 2013

Xu M, Li X, Walsh SW, Zhang Y, Abais JM, Boini KM, Li PL. Intracellular two-phase Ca^{2+} release and apoptosis controlled by TRP-ML1 channel activity in coronary arterial myocytes. *Am J Physiol Cell Physiol* 304: C458–C466, 2013. First published January 2, 2013; doi:10.1152/ajpcell.00342.2012.—Activation of the death receptor Fas has been reported to produce a two-phase intracellular Ca^{2+} release response in coronary arterial myocytes (CAMs), which consists of local Ca^{2+} bursts via lysosomal transient potential receptor-mucolipin 1 (TRP-ML1) channels and consequent Ca^{2+} release from the sarcoplasmic reticulum (SR). The present study was designed to explore the molecular mechanism by which lysosomal Ca^{2+} bursts are coupled with SR Ca^{2+} release in mouse CAMs and to determine the functional relevance of this lysosome-associated two-phase Ca^{2+} release to apoptosis, a common action of Fas activation with Fas ligand (FasL). By confocal microscopy, we found that transfection of CAMs with TRP-ML1 small interfering (si)RNA substantially inhibited FasL (10 ng/ml)-induced lysosome Ca^{2+} bursts and consequent SR Ca^{2+} release. In contrast, transfection of CAMs with plasmids containing a full-length TRP-ML1 gene enhanced FasL-induced two-phase Ca^{2+} release. We further demonstrated that FasL significantly increased the colocalization of the lysosomal marker Lamp1 with ryanodine receptor 3 and enhanced a dynamic trafficking of lysosomes to the SR. When CAMs were treated with TRP-ML1 siRNA, FasL-induced interactions between the lysosomes and SR were substantially blocked. Functionally, FasL-induced apoptosis and activation of calpain and calcineurin, the Ca^{2+} sensitive proteins that mediate apoptosis, were significantly attenuated by silencing TRP-ML1 gene but enhanced by overexpression of TRP-ML1 gene. These results suggest that TRP-ML1 channel-mediated lysosomal Ca^{2+} bursts upon FasL stimulation promote lysosome trafficking and interactions with the SR, leading to apoptosis of CAMs via a Ca^{2+}-dependent mechanism.

signaling lysosomes; transient receptor potential channel; Ca^{2+} mobilization; programmed cell death

LYSOSOME-MEDIATED SIGNALING is a novel mechanism that regulates intracellular Ca^{2+} levels in a variety of mammalian cells (15, 18). It has been reported that lysosomes contain high levels of Ca^{2+}, which serve as an important intracellular Ca^{2+} store as does the sarcoplasmic reticulum (SR; Ref. 9). In response to different physiological and pathological stimulations, lysosomal Ca^{2+} can be mobilized or released to mediate molecular trafficking or recycling and to control vesicular fusion events associated with lysosomes (15, 19, 22). Recently, this lysosomal Ca^{2+} release is found to be mediated by transient receptor potential-mucolipin 1 (TRP-ML1) channel, a *Mcoln1* gene product (26, 27, 31, 37, 39). In this regard, we have reported that TRP-ML1 channels in lysosomes of arterial smooth muscle cells are permeable to Ca^{2+} and importantly participate in the Ca^{2+} responses to agonists such as endothelin-1 (ET-1) and Fas ligand (FasL; Refs. 37–39), which are characterized by a two-phase intracellular Ca^{2+} release. It has been indicated that the Ca^{2+} releases via lysosomal TRP-ML1 channels and from the SR constitute the first and second phase of the Ca^{2+} response to these agonists, respectively.

Although Ca^{2+}-induced Ca^{2+} release (CICR) has been demonstrated to couple TRP-ML1 channel-mediated lysosomal Ca^{2+} bursts (the 1st phase) to the Ca^{2+} release from the SR (the 2nd phase; Refs. 4, 38), this CICR is temporally very different from the classical CICR because it has a long time delay from the first to second phase of the Ca^{2+} release. It remains unknown how this long time delay between two phases of the Ca^{2+} release occurs. Given that lysosomes can be clustered and traffic toward different organelles within cells (12), it is possible that lysosomal trafficking activated by its Ca^{2+} bursts moves them to aggregate around the SR. This may form a trigger zone to activate the Ca^{2+} release from the SR as proposed by Kinnear et al. (12). The present study tested this hypothesis by using mouse coronary arterial myocytes (CAMs), and FasL as a potent stimulator of the two-phase Ca^{2+} release in CAMs was used to determine whether TRP-ML1-mediated Ca^{2+} release stimulates lysosome trafficking to the SR, where a large release of Ca^{2+} is triggered.

The present study also determined the physiological or pathological relevance of this TRP-ML1 channel-mediated two-phase Ca^{2+} release. It is well known that FasL is a type II transmembrane protein that belongs to the tumor necrosis factor (TNF) superfamily, which can induce apoptosis by binding to its receptor, Fas (8). However, it remains unknown whether FasL-induced apoptosis of CAMs is associated with its action on the two-phase intracellular Ca^{2+} release mediated by TRP-ML1 channels. Previous studies have indicated that severe Ca^{2+} dysregulation may promote cell necrosis while controlled intracellular Ca^{2+} increases induced by mild insults can promote apoptosis (17, 25). We therefore hypothesized that FasL-induced lysosomal Ca^{2+} bursts and consequent global Ca^{2+} increase may promote apoptosis in CAMs, in which activation of TRP-ML1 channels may play a critical role due to its triggering action in the two-phase Ca^{2+} response to FasL stimulation. To test this hypothesis, we used flow cytometry to address the role of TRP-ML channels in FasL-induced apoptosis in CAMs. By biochemical analysis, we also determined the activity of relevant proteases to apoptosis in CAMs with and without inhibition of TRP-ML1 channel activity or its gene

Address for reprint requests and other correspondence: P.-L. Li, Dept. of Pharmacology and Toxicology, Medical College of Virginia, Virginia Commonwealth Univ., 1220 East Broad St., P.O. Box 980613, Richmond, VA 23298 (e-mail: pli@vcu.edu).

silencing and overexpression. Our findings support the view that FasL induces apoptosis in CAMs through activation of lysosomal TRP-ML1 channels and consequent two-phase intracellular Ca^{2+} release in these cells.

MATERIALS AND METHODS

Isolation and culture of mouse CAMs. Mice were purchased from Jackson Laboratory. Eight-week-old male and female mice were used in these experiments. All experimental protocols were reviewed and approved by the Institutional Animal Care and Use Committee of the Virginia Commonwealth University. Mouse CAMs were isolated from mice as previously described (30). In brief, mice were deeply anesthetized with an intraperitoneal injection of pentobarbital sodium (25 mg/kg). Their heart was excised with an intact aortic arch and immersed in a petri dish filled with ice-cold Krebs-Henseleit (KH) solution (20 mM HEPES, 128 mM NaCl, 2.5 mM KCl, 2.7 mM $CaCl_2$, 1 mM $MgCl_2$, and 16 mM glucose at pH 7.4). A 25-gauge needle filled with HBSS (in mM: 5.0 KCl, 0.3 KH_2PO_4, 138 NaCl, 4.0 $NaHCO_3$, 0.3 $Na_2HPO_4 \cdot 7H_2O$, 5.6 D-glucose, and 10.0 HEPES, with 2% antibiotics) was inserted into the aortic lumen opening while the whole heart remained in the ice-cold buffer solution. The opening of the needle was inserted deep into the heart close to the aortic valve and tied in place with the needle tip as close to the base of the heart as possible. The infusion pump started with a 20-ml syringe containing warm HBSS through an intravenous extension set at a rate of 0.1 ml/min for 15 min. HBSS was replaced with warm enzyme solution (1 mg/ml collagenase type I, 0.5 mg/ml soybean trypsin inhibitor, 3% BSA, and 2% antibiotic-antimycotic), which was flushed through the heart at a rate of 0.1 ml/min. Perfusion fluid was collected at 30-, 60-, and 90-min intervals. At 90 min, the heart was cut with scissors, and the apex was opened to flush out the cells that collected inside the ventricle. The fluid was centrifuged at 1,000 rpm for 10 min, the cell-rich pellets were mixed with the media described below, and the cells plated on 2% gelatin-coated six-well plates and incubated in 5% CO_2-95% O_2 at 37°C. Advanced DMEM with 10% FBS, 10% mouse serum, and 2% antibiotics was then used to suspend isolated cells for the first stage culture. The medium was replaced three days later and then once or twice each week until the cells grew to confluence. Mouse CAMs were identified according to their morphology, immunohistological staining, Western blot analysis of marker proteins, and flow cytometric characteristics as described previously (33).

RNA interference of TRP-ML1 in CAMs. Specific gene silencing was achieved by transfection of double-stranded small interfering (si)RNA targeting TRP-ML1 (Accession No.: BC118374) consisting of 5′-CAGCUUCCGGCUCCUG-3′. The scrambled small RNA (5′-AATTCTCCGAACGTGTCACGT-3′) was also confirmed as nonsilencing double-stranded RNA and used as a control in the present study. TRP-ML1 cDNA was prepared and used as we described previously (39). Transfection of siRNA or cDNA was performed using the siLentFect Lipid Reagent or TransFectin Lipid Reagent (Bio-Rad) according to the manufacturer's instructions (40). The efficiency of TRP-ML1 silencing was assessed by Western blot and real-time PCR analyses. The TRP-ML1 antibody was purchased from Santa Cruz Biotechnology (sc-48745).

Fluorescent confocal microscopic measurement of intracellular Ca^{2+} and lysosome Ca^{2+} release. As described in our previous study (38), subconfluent CAMs in 35-mm cell culture dishes were loaded with the Ca^{2+}-sensitive dye fluo-4 (5 μM) in HBSS and then incubated at room temperature for 20 min. The fluo 4-loaded CAMs were then bathed with Ca^{2+}-free HBSS buffer containing 1 mM EGTA. Ca^{2+} imaging was performed using a laser scanning confocal microscope (Olympus Fluoview System, version 5.0, FV300), which consists of an Olympus BX61WI inverted microscope with an Olympus Lumplan F1×60, 0.9 numerical aperture, and water-immersion objective. Pseudocolor Ca^{2+}/fluo-4 fluorescence images were acquired at 488-nm excitation and >510-nm emission in the XYT recording mode with a speed of 2 frames/s. The Ca^{2+}/fluo-4 fluorescence intensity was analyzed with Fluoview version 5.0 software. The ratio of Ca^{2+}-dependent fluorescence intensity to that at the basal level was quantified as the intracellular Ca^{2+} response.

To detect lysosome Ca^{2+} release, subconfluent CAMs in 35-mm cell culture dishes were incubated with dextran-conjugated tetramethylrhodamine (Rho; 1 mg/ml; Molecular Probes) for 4 h in advanced DMEM medium containing 10% FBS at 37°C, 5% CO_2, followed by a 20-h chase in dye-free medium for lysosomes loaded with Rho as previously described (5, 38). After being washed with HBSS buffer three times, the Rho-loaded cells were then incubated with the Ca^{2+}-sensitive dye fluo-4 at a concentration of 5 μM. Ca^{2+} release and lysosome trace recordings were performed in the presence of FasL (10 ng/ml) with or without the pretreatment with TRP-ML1 siRNA and cDNA as described above. Lysosome/Rho (Lyso/Rho) fluorescence images were acquired at 568-nm excitation and 590-nm emission. The colocalization coefficiency of Ca^{2+}/fluo-4 and Lyso/Rho was analyzed with Image-Pro Plus 6.0 software (41).

Confocal microscopic colocalization of the lysosome marker Lamp1 with ryanodine receptor 3 in CAMs. For dual-staining detection of the colocalization of Lamp1 with ryanodine receptor 3 (RyR3), the CAMs were first incubated with FITC-labeled anti-Lamp1 antibody and then with rabbit anti-RyR3 polyclonal antibody (1:200; Santa Cruz, CA), followed by incubation with Texas red-conjugated anti-rabbit (1:500; Molecular Probes, Carlsbad, CA) secondary antibody. An excitation/emission wavelength of 570/625 nm was used for confocal microscopy of Texas red, and the colocalization was visualized by confocal microscopy.

Confocal microscopy of lysosome trafficking toward the SR. CAMs (2×10^4/ml) cultured in 35-mm dish were incubated with organelle lights SR-RFP (12 μl/well; Invitrogen) in complete cell medium at 37°C for 16 h. Then, the medium from the dish was removed and prewarmed (37°C) medium containing LysoTracker Green (50 nM; Invitrogen) was added. The cells were incubated for 30 min under growth conditions, and the loading solution was replaced with the fresh medium (same volume). The confocal fluorescent microscopic recording was conducted with an Olympus Fluoview System. The fluorescent images for lysosomes (LysoTracker Green) and SR (SR-RFP) of the CAMs were continuously recorded at an excitation/emission (nm) of 504/511 and 488/530 by using XYT recording mode with a speed of 2 frames/s for 15 min. The pixels between lysosomes and SR were measured by the Image Pro-Plus software. The relative value to basal pixels was calculated as the distance between lysosome and SR.

Flow cytometric detection of cell apoptosis. Apoptosis of CAMs was detected using an annexin V-propidium iodide (PI) double staining kit (Sigma, St. Louis, MO) according to the manufacturer's instructions. CAMs were trypsinized and collected by centrifugation at 500 *g* for 8 min at room temperature. The cells were washed in cold (2–8°C) PBS and then subjected to another centrifugation. Then, the cells were resuspended in the annexin V-PI reagent for 10 min at a concentration of 1×10^6 cells/100 μl. After resuspension and washing with the reaction, the cells were detected using a flow cytometer (GUAVA, Hayward, CA) within 1 h. Annexin V-positive–PI-negative cells were considered as apoptotic. The percentage of cells to total cells was calculated as the rate of apoptotic cells (see Fig. 6*A*, *bottom right*).

Assay of calpain and calcineurin activity. Fluorogenic substrate assays were performed with Suc-Leu-Leu-Val-Tyr-AMC (Suc-LLVY), a membrane-permeable calpain-specific fluorogenic substrate as previously described (24). Proteolytic hydrolysis of the peptidyl-7-amilorideno bond liberates the highly fluorescent 7-amilorideno-4-methylcoumarin (AMC) moiety. Cellular fluorescence was quantified by fluorometry with 360-nm excitation and 460-nm emission filters. Standard curves were generated with free AMC for each experiment. For measurements of calpain activity, CAMs were plated at 10^5 cells in 200 μl medium per well in 96-well plates and incubated for 24 h at

37°C. The medium was removed from the adherent cell layer, and cells were then treated with FasL. After a 15-min incubation at 37°C, 200 μl of assay buffer (115 mM NaCl, 1 mM KH_2PO4, 5 mM KCl, 2 mM $CaCl_2$, 1.2 mM $MgSO_4$, and 25 mM sodium HEPES buffer at pH 7.4) were added to all wells. To determine the maximal calpain activity under our experimental conditions, the Ca^{2+} ionophore A23187 (5 mM) was added to representative wells. As an additional control to ensure that fluorescence activity was calpain specific, aLLN (50 mM) was added to representative wells for each condition. Other controls included aLLN alone, A23187 alone, and FasL alone in the absence of cells. Suc-LLVY substrate (62.5 mM) was added to each well at the start of the assay. The plates were incubated at 37°C in the fluorometer, and fluorescence was measured at 5-min intervals starting immediately after the addition of substrate. Calpain activity was calculated as mean fluorescence ± SE. For conditions with the Ca^{2+} ionophore A23187, the inherent fluorescence of this compound (determined from wells containing A23187 in the absence of cells) was subtracted from the total measured fluorescence to accurately represent maximal calpain activity. For comparison of calpain activity at 120 min, the net calpain activity under FasL treatment was calculated by subtracting the residual activity in the presence of calpain inhibitor.

In addition, calcineurin activity was determined according to manufacturer's kit (BML-AK816; Enzo). The detection of free-phosphate in the supernatant by colorimetric assay represented the activity of calcineurin in mouse CAMs.

Statistics. Data are presented as means ± SE. Significant differences between and within multiple groups were examined using ANOVA for repeated measures, followed by Duncan's multiple-range test. A Students' *t*-test was used to detect significant differences between two groups. $P < 0.05$ was considered statistically significant.

RESULTS

Efficiency of TRP-ML1 siRNA or cDNA on TRP-ML1 channel expression. RT-PCR and Western blot analysis were used to demonstrate the efficiency of TRP-ML1 gene silencing by siRNA transfection or overexpression of TRP-ML1 gene by introduction of a full-length TRP-ML1 gene in CAMs. As shown in Fig. 1*A*, the mRNA level of TRP-ML1 was reduced by 72.4% after transfection of TRP-ML1 siRNA but increased by 1.43 fold after TRP-ML1 gene transfection in CAMs. Furthermore, Western blot analysis as presented in Fig. 1, *B* and *C*, showed that the protein expression of TRP-ML1 decreased by 63.5% and increased by 97.6% by TRP-ML1 siRNA or a full-length gene transfection respectively.

RNA interference of TRP-ML1 blocked Fas activation-induced lysosomal Ca^{2+} bursts. To determine the role of lysosomal TRP-ML1 channels in the two-phase Ca^{2+} release, fluorescent imaging analysis was conducted to test the effects of TRP-ML1 inhibition on the Ca^{2+} release in intact CAMs in response to FasL. In Fig. 2*A* (taken from the Supplemental Movies; Supplemental Material for this article is available online at the *Am J Physiol Cell Physiol* website), typical Fluo4-Ca^{2+} images demonstrate a two-phase transient Ca^{2+} release pattern in CAMs upon FasL stimulation, consisting of an early Ca^{2+} release at 4.5 min (the 1st phase, red dots in the image), followed by a global increase in intracellular Ca^{2+} at 10 min (the 2nd phase). When CAMs were transfected with TRP-ML1 siRNA, FasL-induced two-phase Ca^{2+} increases were almost completely blocked. Summarized data of FasL-induced Ca^{2+} fluorescent intensity in the first and second phases in CAMs with scramble sRNA were 340 ± 23.4 and 519.3 ± 31.3, respectively. In CAMs with TRP-ML1 siRNA transfection, Ca^{2+} fluorescent intensity in the first and second phases decreased to 241.2 ± 18.2 and 273.5 ± 30.6, respectively. The relative fluorescent intensity normalized to basal condition is presented in Fig. 2*B*. In contrast to siRNA, when CAMs were transfected with full-length TRP-ML1 gene, the two-phase Ca^{2+} release was increased compared with mock vector transfection. In contrast to a two-phase Ca^{2+} release induced by FasL, single-phase Ca^{2+} release induced by oxotremorine (RyR-mediated Ca^{2+} release agonist) or U46619 [inositol 1,4,5-trisphosphate (IP_3) receptor-mediated Ca^{2+} release agonist] was not altered in CAMs when their TRP-ML1 channel activities were inhibited (data not shown).

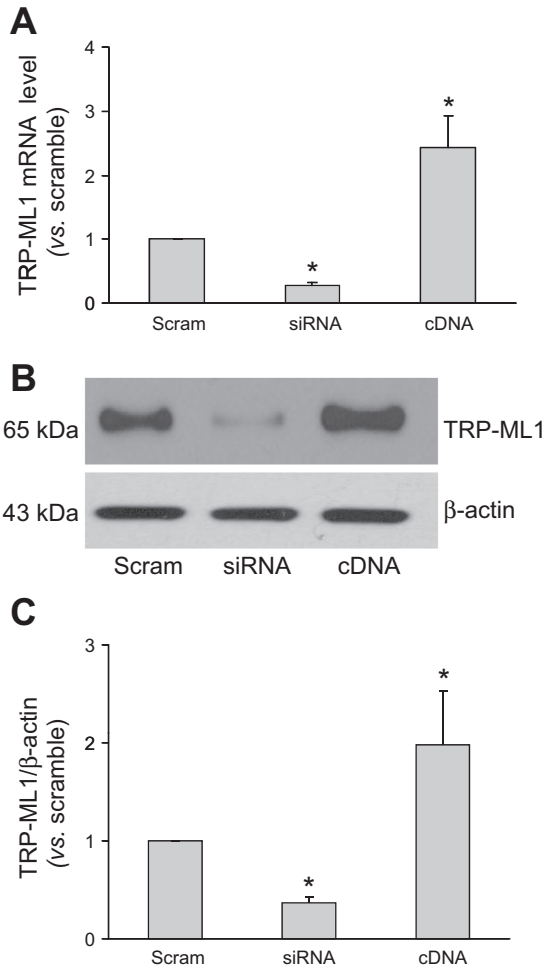

Fig. 1. Efficiency of transient potential receptor-mucolipin 1 (TRP-ML1) small interfering (si)RNA or cDNA on TRP-ML1 channel expression. *A*: TRP-ML1 mRNA expression with transfection of TRP-ML1 siRNA or cDNA plasmids into mouse coronary arterial myocytes (CAMs). *B*: representative Western blot gel document showing the expression of TRP-ML1 in CAMs transfected with scramble sRNA, TRP-ML1 siRNA, or cDNA. *C*: summarized data showing the intensity of detected TRP-ML1 proteins on Western blot analysis. ($n = 6$; $^*P < 0.05$ vs. scramble sRNA-transfected CAMs).

TRP-ML1 channels mediated Fas activation-induced lysosomal Ca^{2+} release. Another method used to detect lysosomal Ca^{2+} release was related to localization of Ca^{2+} around lysosomes by confocal microscopy. As shown in Fig. 3*A*, Ca^{2+} release regions in the first phase (4.5 min) were well colocalized with lysosomes as shown by yellow spots formed by green fluo-4 signals with rhodamine-red lysosomal marker. Summarized data showed that the colocalization coefficient of Ca^{2+} by

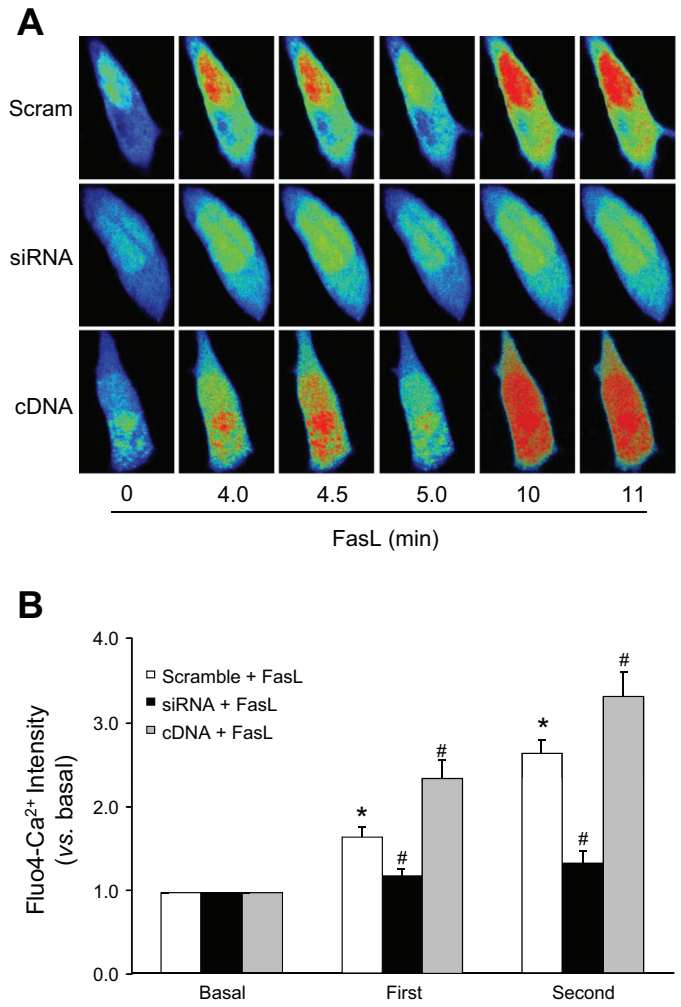

Fig. 2. Effects of TRP-ML1 channel gene silencing or overexpression on Fas ligand (FasL)-induced lysosomal Ca^{2+} bursts and Ca^{2+} release from the sarcoplasmic reticulum (SR) of mouse CAMs. *A*: representative Fluo4-Ca^{2+} imaging record showed an early Ca^{2+} release (1st phase, at 4.5 min; red spots in the image), followed by a global increase in intracellular Ca^{2+} (red cytosol; 2nd phase, at 10 min) upon FasL (10 ng/ml) stimulation in CAMs before and after transfection of TRP-ML1 siRNA or cDNA. *B*: summarized data showing the effects of TRP-ML1 siRNA or its overexpression on FasL-induced 2-phase Ca^{2+} release in CAMs. ($n = 6$; $^{*}P < 0.05$ vs. basal condition; $^{\#}P < 0.05$ vs. scramble sRNA-treated CAMs with FasL stimulation).

fluo-4 and Lyso by Rho significantly increased by 89.5% in FasL-stimulated CAMs compared with basal condition. Transfection of CAMs with TRP-ML1 siRNA resulted in a significant inhibition of FasL-induced local Ca^{2+} release (Fig. 3*B*).

Lysosomal Ca^{2+} release via TRP-ML1 channel increased the colocalization of Lamp1 and RyR3. Lysosomal TRP-ML1 Ca^{2+} release may stimulate lysosome trafficking into the proximity of the SR where Ca^{2+} release is triggered. To test this possibility, we stained CAMs with FITC-labeled anti-Lamp1 antibody and TR-conjugated anti-RyR3 antibody and examined their colocalization upon FasL stimulation. Lamp1 is a lysosomal marker protein belonging to a type 1 integral membrane protein and is highly expressed in lysosomal membranes (2). RyR3 is a predominant receptor subtype on the SR of vascular smooth muscle cells (11). In Fig. 4*A*, yellow dots in the overlaid images represent a colocalization of Lamp1 and RyR3. Under the control condition, only a few yellow dots were detected; however, FasL stimulation significantly increased yellow dots to become intracellular patches, suggesting an increased colocalization of Lamp1 with RyR3 representing the interaction between the lysosomes and SR. The colocalization coefficient of Lamp1 and RyR3 were summarized in Fig. 4*B*, showing that FasL significantly increased the interaction between the lysosomes and SR, which was abolished by TRP-ML1 siRNA transfection.

Lysosomal Ca^{2+} release via TRP-ML1 channels increased the lysosome trafficking to the SR. To dynamically observe the lysosome trafficking to the SR in live cells, we labeled the lysosomes with LysoTracker Green and the SR with SR-RFP, respectively. LysoTracker Green is a green fluorescent dye that stains acidic compartments in live cells with excitation/emis-

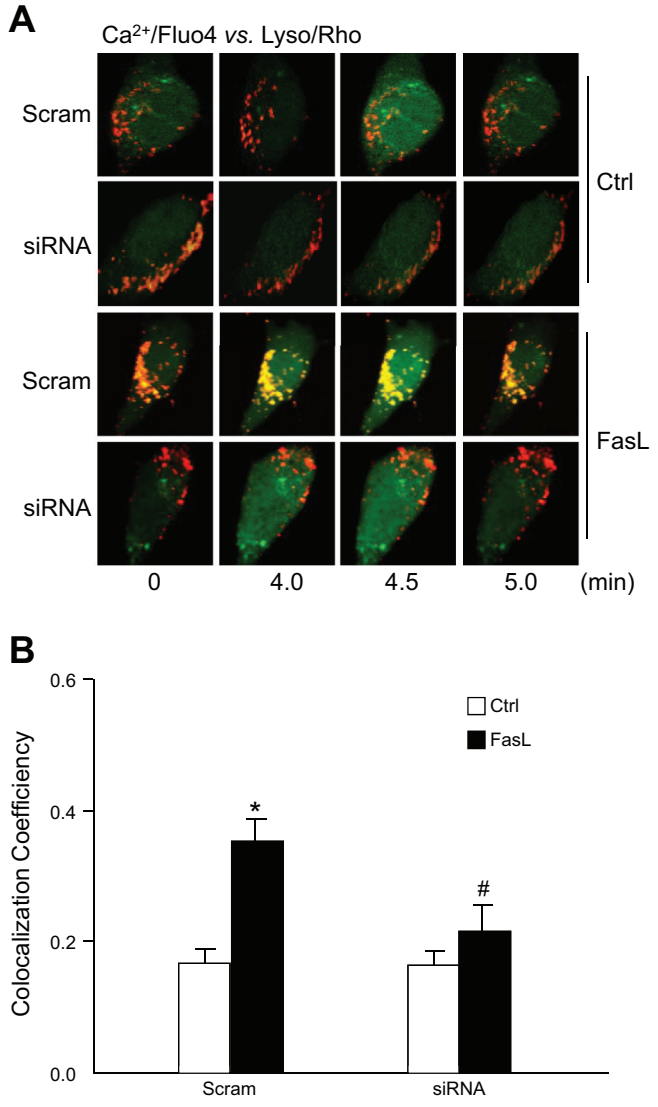

Fig. 3. Confocal microscopic detection of FasL-induced local Ca^{2+} release from lysosomes in mouse CAMs before and after silencing TRP-ML1 channel gene. *A*: representative confocal microscopic images showing the Ca^{2+} release locations in the first phase (4.5 min) colocalized with lysosomes (red image) in FasL-stimulated CAMs. *B*: summarized data showing the colocalization coefficiency of Ca^{2+}/fluo-4 with Lyso/Rho signals. ($n = 6$; $^{*}P < 0.05$ *vs.* scramble sRNA transfected CAMs; $^{\#}P < 0.05$ vs. scramble sRNA-treated CAMs with FasL stimulation).

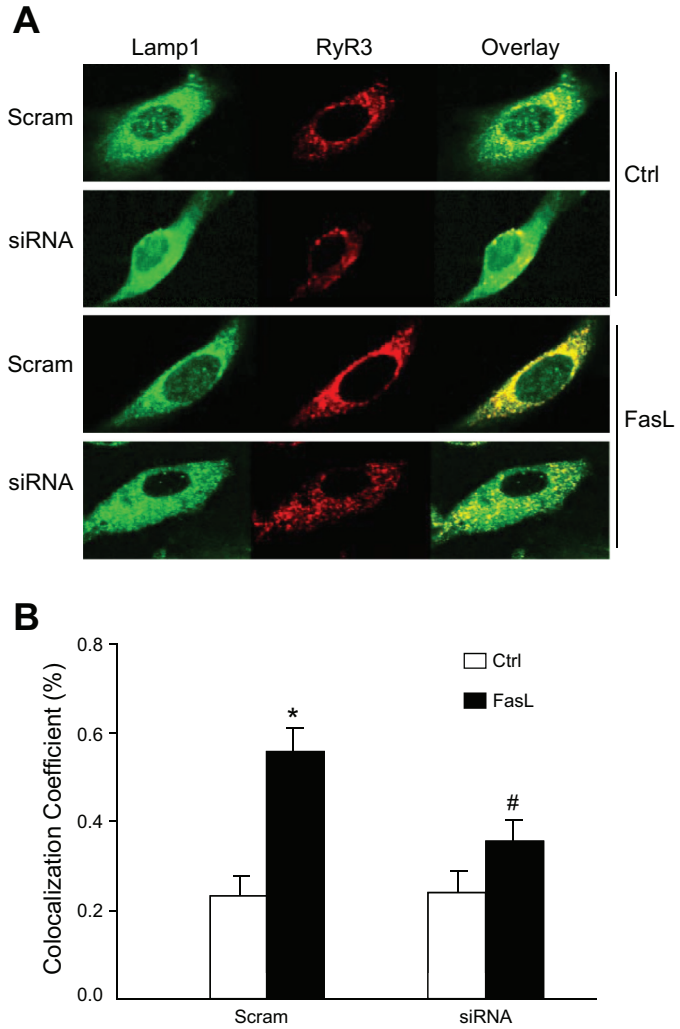

Fig. 4. Colocalization of the lysosomal marker Lamp1 with SR marker, RyR3 in mouse CAMs upon FasL stimulation before and after silencing TRP-ML1 gene. *A*: representative confocal microscopic images showing colocalization of Lamp1 and ryanodine receptor 3 (RyR3). Under the control condition, little yellow dots were detected, but FasL significantly increased yellow staining. *B*: summarized results showing the colocalization coefficient of Lamp1 with RyR3 in CAMs treated with scramble sRNA or TRP-ML1 siRNA. (n = 6; $^{*}P < 0.05$ vs. scramble RNA treated CAMs; $^{\#}P < 0.05$ vs. scramble sRNA-treated CAMs with FasL stimulation).

sion wavelength of ~504/511 nm. The SR was labeled with organelle Lights SR-RFP, which is a TagRFP fused to the SR signal sequence of calreticulin and KDEL (SR retention signal). As shown in Fig. 5*A*, typical fluorescent images of CAMs were taken at 0, 1, 3, 5, and 7 min in control or FasL-treated cells. Under control condition, lysosomes were located near SR strands. FasL induced an obvious trafficking of lysosomes toward the SR (as showed by arrows), as confirmed by the decreased distance between the lysosomes and SR in a time-dependent manner (Fig. 5*B*). The summarized data in Fig. 5*B* showed that the dynamic movement of lysosomes to the SR was decreased after the TRP-ML1 siRNA transfection.

TRP-ML1 Ca^{2+} release contributed to FasL-induced apoptosis. First, we used annexin V-PI double-stained CAMs to measure apoptosis and found that FasL doubled apoptotic CAMs compared with vehicle treatment (Fig. 6, *A* and *B*). When CAMs were transfected with TRP-ML1 siRNA, FasL-induced apoptosis was markedly suppressed by 45.7%. However, FasL-induced apoptosis was markedly increased by TRP-ML1 overexpression in CAMs (58.8%). Since calpain and calcineurin are two important effectors of intracellular Ca^{2+}, which initiate apoptosis (28, 34), we examined whether they are involved in FasL-induced apoptosis in CAMs. With the use of cyclosporin A and PD150606, the selective inhibitor of calcineurin and calpain, respectively, we demonstrated that FasL-induced apoptosis was attenuated by 62.8% by cyclosporin A and by 40.6% by PD150606, suggesting that both calcineurin and calpain are indeed involved in FasL-induced apoptosis in CAMs (Fig. 6*C*).

Calpain and calcineurin activity in CAMs. We further determined whether the activities of calpain and calcineurin can be altered by increase or decrease in TRP-ML1 gene expres-

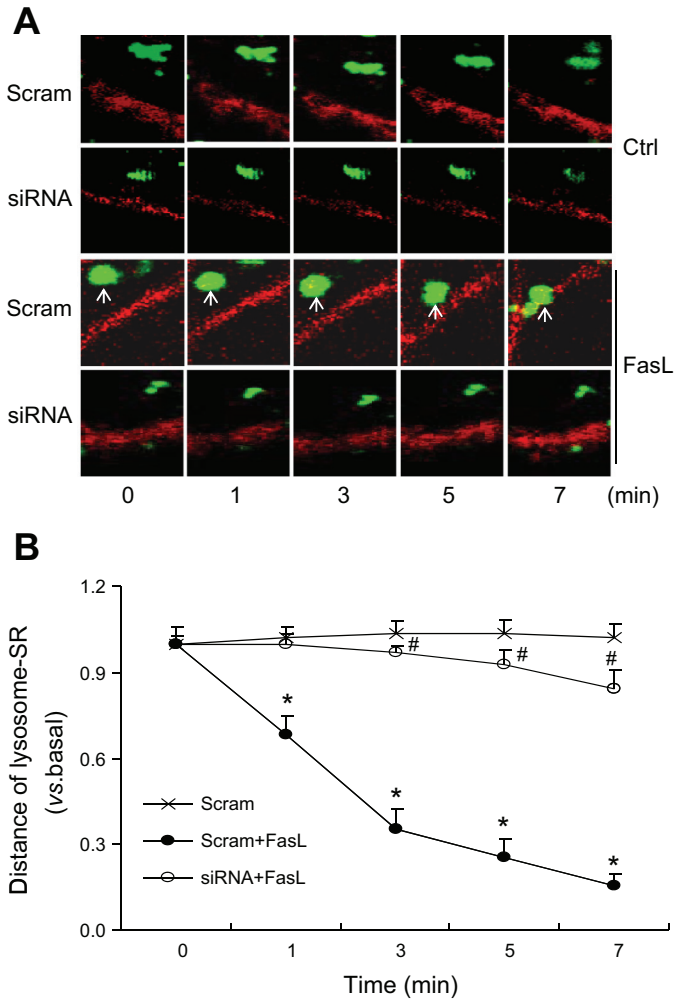

Fig. 5. Monitoring of lysosome trafficking toward the SR in mouse CAMs before and after silencing TRP-ML1 channel. *A*: typical dynamically recorded fluorescent images showing lysosome trafficking. Under the rest condition, lysosomes (green) were located near SR strands (red). When the CAM received FasL (10 ng/ml) stimulation, a clear interaction between the lysosome and SR was observed repeatedly (as shown by arrows), which was inhibited after silencing TRP-ML1 gene. *B*: distance measurement of lysosomes to the SR by counting the pixels of lysosome movements toward the SR. FasL significantly decreased the distance with time, which was inhibited by TRP-ML1 siRNA (n = 4; $^{*}P < 0.05$ vs. scramble RNA-treated CAMs; $^{\#}P < 0.05$ vs. scramble sRNA-treated CAMs with FasL stimulation).

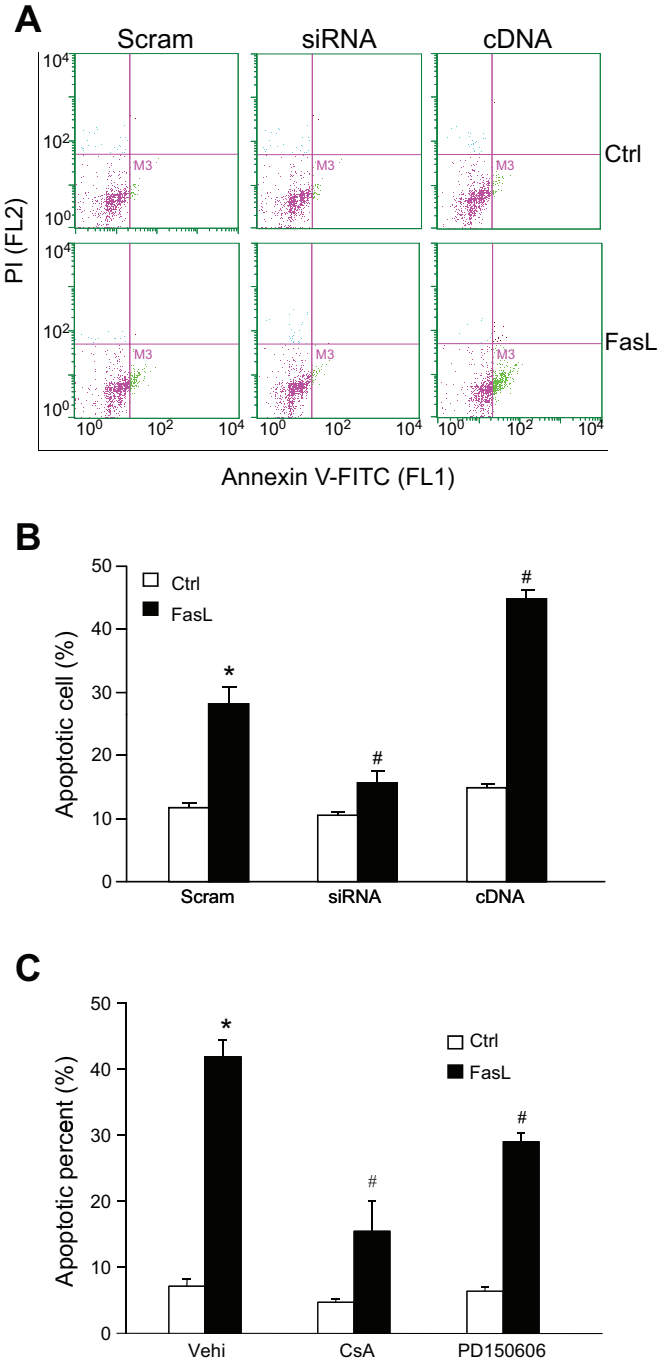

Fig. 6. Role of TRP-ML1-mediated Ca^{2+} signaling in FasL-induced apoptosis of mouse CAMs. *A*: representative plots showing the apoptotic CAM populations (the *top right* and *bottom right* of the plots) sorted by flow cytometry after they were double-stained with FITC-annexin V and propidium iodide (PI). *B*: summarized data showing the effects of TRP-ML1 gene silencing or overexpression. *C*: summarized data showing the effects of the calcineurin inhibitor cyclosporin A (CsA; 10 μM) and the calpain inhibitor PD150606 (100 μM) on FasL-induced apoptosis ($n = 6$; $^*P < 0.05$ vs. control or scramble RNA treated CAMs; $^{\#}P < 0.05$ vs. scramble sRNA-treated CAMs with FasL stimulation).

sion. As shown in Fig. 7*A*, FasL-treated CAMs had much higher calpain activity than control CAMs. This FasL-induced calpain activation was significantly attenuated by TRP-ML1 gene silencing. In contrast, calpain activity was markedly increased by TRP-ML1 gene overexpression in CAMs. Figure 7*B* shows that FasL tripled calcineurin activity in scramble RNA transfected CAMs and that this FasL-induced enhancement of calcineurin activity was markedly attenuated by TRP-

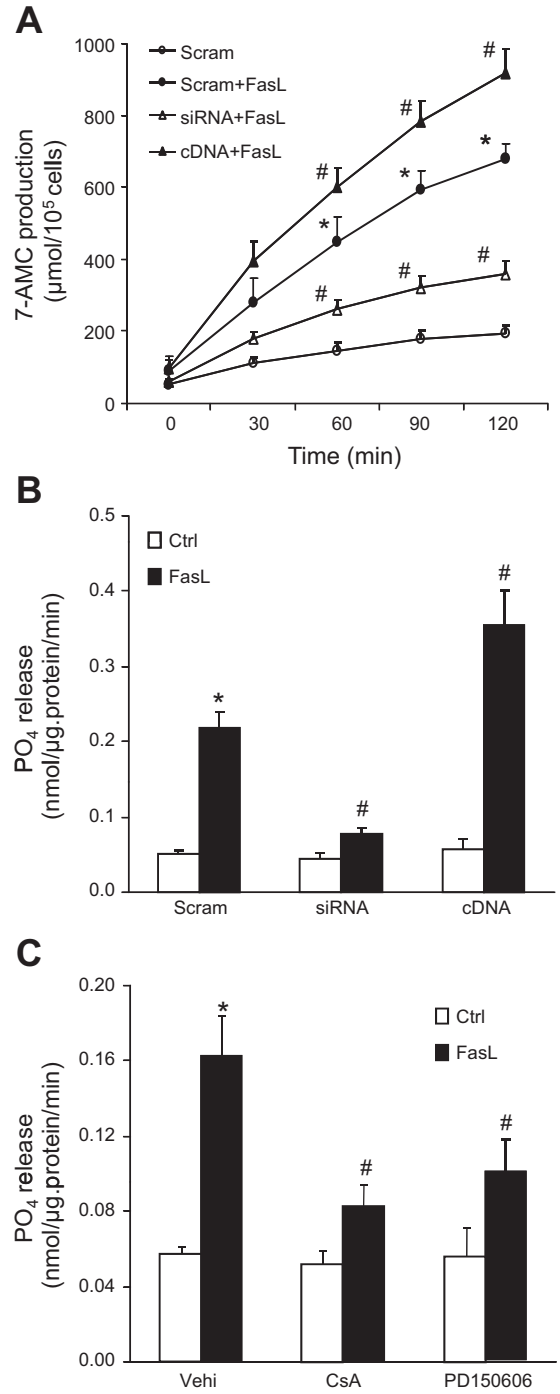

Fig. 7. Role of TRP-ML1 channel in FasL-induced activation of calpain and calcineurin in mouse CAMs. *A*: FasL-induced activation of calpain in CAMs with or without TRP-ML1 gene silencing. $^*P < 0.05$ vs. control; $^{\#}P < 0.05$ vs. CAMs treated with TRP-ML1 siRNA ($n = 6$). *B*: FasL-induced activation of calcineurin in CAMs with or without TRP-ML1 gene silencing or overexpression. *C*: FasL-induced activation of calcineurin in CAMs treated with vehicle, cyclosporin A (10 μM), or PD150606 (100 μM; $n = 6$; $^*P < 0.05$ vs. control or scramble RNA transfected cells; $^{\#}P < 0.05$ vs. vehicle or scramble sRNA-treated CAMs with FasL stimulation).

ML1 gene silencing but significantly enhanced by TRP-ML1 gene overexpression. In the presence of cyclosporin A or PD150606, the FasL-induced calcineurin activation in CAMs was markedly suppressed (Fig. 7*C*).

DISCUSSION

The present study provides the first direct evidence that TRP-ML1 channel activity is implicated in FasL-induced lysosomal Ca^{2+} bursts and consequent global Ca^{2+} increase due to its mobilization from the SR. This TRP-ML-1-mediated two-phase Ca^{2+} release is associated with lysosome trafficking toward and interaction with the SR. We also demonstrated that FasL induced apoptosis in CAMs through activation of lysosomal TRP-ML1 channels and associated Ca^{2+} release responses.

Although FasL was previously reported to stimulate lysosomal Ca^{2+} bursts followed by a global increase in intracellular Ca^{2+} concentrations (38), it remains unknown how these lysosomal Ca^{2+} bursts are produced upon FasL stimulation and what mechanism mediates the coupling of lysosomal Ca^{2+} bursts to the SR Ca^{2+} release. The present study first determined whether lysosomal TRP-ML1 channel activity is involved in FasL-induced two-phase intracellular Ca^{2+} release and then tested whether this action of lysosomal TRP-ML1 channels is attributed to lysosome trafficking toward the SR, where a large Ca^{2+} release is activated to cause global Ca^{2+} increases in CAMs. We demonstrated that FasL-induced lysosomal Ca^{2+} release and consequent Ca^{2+} release from the SR were blocked or enhanced, respectively, by silencing or overexpression of TRP-ML1 gene in mouse CAMs. This supports the view that lysosomal TRP-ML1 channel is critically implicated in the Ca^{2+} response to FasL stimulation. Similar to the inhibitory effect of TRP-ML1 siRNA, pharmacological intervention to TRP-ML1 channel activity with amiloride or lanthanum also significantly attenuated FasL-induced two-phase Ca^{2+} release in CAMs (data were not shown). However, both pharmacological interventions and RNA interference of the TRP-ML1 gene had no effect on Ca^{2+} release induced by oxotremorine, an agonist that uses RyR-mediated Ca^{2+} signaling pathway or by U46619, a typical agonist using IP_3 receptor-mediated Ca^{2+} signaling mechanism. These results suggest that activation of TRP-ML1 channels is specific to mediate FasL-induced signal transduction through a two-phase Ca^{2+} release. To our knowledge, these results are the first time to link FasL action to lysosomal TRP-ML1 channel-mediated signaling.

Since lysosomal Ca^{2+} concentrations are maintained in part by the proton gradient across lysosome membrane (9) and V-H^+-ATPase as a lysosome resident proton pump to maintain an acidic milieu in the lysosomal lumen may drive Ca^{2+} uptake into the lysosomes by Ca^{2+}/H^+exchange, inhibition of V-H^+-ATPase may also cause the depletion of lysosomal Ca^{2+} storage and thereby lead to no Ca^{2+} release response via TRP-ML1. We also tested this possibility in CAMs. Similar to TRP-ML1 gene silencing, FasL-induced Ca^{2+} release from lysosomes and subsequently from the SR was substantially blocked by pretreatment of CAMs with bafilomycin, a specific inhibitor of lysosomal V-H^+-ATPase (Supplemental Fig. S1). This further supports the view that FasL-induced Ca^{2+} release response is associated with lysosomal Ca^{2+} store. However, these experiments using bafilomycin may not exclude the role of other lysosomal Ca^{2+} release channels such as two-pore channels (TPCs). It has been reported that TPCs are present in the endo/lysosomal system and they may be a Ca^{2+} release channel in lysosomes (22, 29). However, the present study showed that the siRNA of TPC2, a major TPC reported to mediate lysosomal Ca^{2+} release, had no inhibitory effect on FasL-induced Ca^{2+} release from lysosomes of CAMs (Supplemental Fig. S2). In addition, a most recent study reported that TPC in endo/lysosomes primarily functions as a sodium channel (31). Taken together, all these results indicate that lysosomal TRP-ML1 channels mediate FasL-induced two-phase intracellular Ca^{2+} release in mouse CAMs.

We next addressed how Ca^{2+} bursts produced by lysosomal TRP-ML1 channels trigger the Ca^{2+} release from the SR. It has been reported that CICR triggers release of Ca^{2+} from the SR without the simultaneous action of other activating processes in a variety of mammalian cells (7, 14). Traditionally, CICR produces global intracellular Ca^{2+} increase in milliseconds or seconds and is then inactivated. However, recent studies in our laboratory and by others showed that a slow CICR process is involved in the occurrence of the second phase of Ca^{2+} increase in different cells in response to different agonists such as ET-1 and FasL (4, 12, 37–38). This slow CICR is featured by a delay of minutes after the first phase of Ca^{2+} bursts from lysosomes, which is temporally very different from the classic CICR. Given the great mobility of lysosomes within cells, it is possible that Ca^{2+} bursts from individual lysosomes may not be enough to trigger the SR Ca^{2+} release, but such Ca^{2+} bursts are able to stimulate lysosome trafficking toward the SR. When increasing numbers of lysosomes aggregate around the SR, local Ca^{2+} concentrations increase to reach a threshold for activation of RyR or IP_3 receptor, thereby resulting in a large SR Ca^{2+} release. In the present study, we first observed an increased colocalization of the lysosomal marker Lamp1 with RyR3 when CAMs were stimulated by FasL. Then, a dynamic movement of lysosomes toward the SR was demonstrated upon FasL stimulation. Importantly, inhibition of TRP-ML1 channel activity or silencing its gene blocked the colocalization of Lamp-1 and RyR3 and attenuated the interactions of lysosomes with the SR. These results confirm our hypothesis that lysosomes are trafficking toward the SR upon FasL stimulation and that TRP-ML1 channel activity is critical in such lysosome trafficking, which triggers CICR and leads to a large Ca^{2+} release from the SR. It is obvious that lysosome movement and subsequent accumulation of Ca^{2+} around aggregated lysosomes in the proximity of the SR result in a delay of the second phase of Ca^{2+} release from the SR. This time delay of the Ca^{2+} release from the SR was also observed in a number of other cell types such as starfish eggs, sea urchin eggs, and pancreatic acinar cells (6, 10, 23), which is now attributed to the lysosome trafficking and aggregation around the SR.

The present study also addressed the importance of TRP-ML1 channel activity in the regulation of apoptosis in CAMs. It has been reported that increased cytosolic Ca^{2+} contributes to the activation and progression of apoptosis in response to different death factors such as FasL, TNF-α, and TNF-related apoptosis-inducing ligands (TRAILs; Refs. 1, 3, 17, 25). However, it remains unknown whether the Ca^{2+} release from lysosomes via TRP-ML1 channels plays a role in apoptosis of

CAMs upon activation of death receptors such as Fas. In the present study, using flow cytometry we demonstrated that FasL increased annexin V-positive CAMs, indicating enhanced apoptosis. However, inhibition of TRP-ML1 activity or silencing of the TRP-ML1 gene significantly suppressed, but TRP-ML1 gene overexpression significantly enhanced, FasL-induced apoptosis of CAMs. This role of TRP-ML1 channels in apoptosis of CAMs was also observed by using TRP-ML1 channel blockers, amiloride, and lanthanum. These results suggest that the functional TRP-ML1 channels are the prerequisite for FasL to induce apoptosis in CAMs. Although previous studies have shown that FasL-mediated apoptosis requires Ca^{2+} release from the ER through IP_3 in Jurkat T-lymphoma cells (32), the mechanism mediating FasL-induced activation of IP_3 signaling remains unclear. It is possible that the action of FasL on IP_3 signaling is also due to lysosomal Ca^{2+} bursts associated with the TRP-ML1 activity. In this way, activation of TRP-ML1 channel produces lysosomal Ca^{2+} bursts and consequently leads to CICR associated with lysosome trafficking, resulting in IP_3 receptor activation and the large Ca^{2+} release from the SR.

To further explore the mechanisms by which TRP-ML1 channel-mediated lysosome Ca^{2+} bursts induce apoptosis during activation of Fas, we analyzed the activities of calpain and calcineurin, two Ca^{2+} sensitive apoptosis-activating enzymes. It is well known that calpain is a Ca^{2+}-activated neutral cysteine protease that catalyzes limited proteolysis of substrate proteins (34–36), which directly activates caspases to promote apoptosis with ER stress independent of mitochondrial cytochrome *c* release (20). Calcineurin is a widely distributed protein phosphatase, and it belongs to the protein phosphatase 2B family of Ca^{2+}/calmodulin-dependent serine/threonine protein phosphatases (13). The activation of calcineurin may initiate mitochondrial dysfunction and further stimulate the mitochondria-dependent cell death pathway (16, 21, 28). In the present study, we found that FasL-increased activity of calpain and calcineurin was almost completely inhibited by TRP-ML1 blockers or its siRNA but augmented by overexpression of TRP-ML1 gene. With the use of their selective inhibitors, FasL-induced enhancement of calpain or calcineurin activity was blocked to a similar extent to that induced by TRP-ML1 blockers or siRNA. These results further confirm a novel pathway mediating apoptosis of CAMs, which is associated with activation of lysosomal TRP-ML1 channels and consequent Ca^{2+}-sensitive protease activity.

In summary, we demonstrated that TRP-ML1 channels are importantly implicated in FasL-induced Ca^{2+} release from lysosomes in CAMs. This lysosomal Ca^{2+} burst promotes lysosome trafficking toward the SR, where aggregated lysosomes with more Ca^{2+} bursts interact with the SR, producing a large Ca^{2+} release from the SR via CICR in CAMs. Another important finding of the present study is that TRP-ML1-mediated Ca^{2+} signaling is critical to the apoptosis of CAMs, and its role is attributed to Ca^{2+}-dependent activities of apoptosis-activating enzymes such as calpain and calcineurin. It is concluded that the activation of lysosomal TRP-ML1 channels critically mediates the two-phase Ca^{2+} release in CAMs, which may represent a novel mechanism leading to apoptosis of these cells in response to FasL stimulation.

GRANTS

This work was supported by National Heart, Lung, and Blood Institute Grants HL-091464, HL-075316, and HL-057244.

DISCLOSURES

No conflicts of interest, financial or otherwise, are declared by the author(s).

AUTHOR CONTRIBUTIONS

Author contributions: M.X. and P.-L.L. conception and design of research; M.X. and X.L. performed experiments; M.X. and X.L. analyzed data; M.X. interpreted results of experiments; M.X. prepared figures; M.X. drafted manuscript; M.X., S.W.W., Y.Z., J.M.A., K.M.B., and P.-L.L. edited and revised manuscript; M.X., Y.Z., and P.-L.L. approved final version of manuscript.

REFERENCES

1. **Ayub K, Laffafian I, Dewitt S, Hallett MB.** Ca influx shutdown in neutrophils induced by Fas (CD95) cross-linking. *Immunology* 112: 454–460, 2004.
2. **Barrachina M, Maes T, Buesa C, Ferrer I.** Lysosome-associated membrane protein 1 (LAMP-1) in Alzheimer's disease. *Neuropathol Appl Neurobiol* 32: 505–516, 2006.
3. **Boehning D, van Rossum DB, Patterson RL, Snyder SH.** A peptide inhibitor of cytochrome c/inositol 1,4,5-trisphosphate receptor binding blocks intrinsic and extrinsic cell death pathways. *Proc Natl Acad Sci USA* 102: 1466–1471, 2005.
4. **Boittin FX, Galione A, Evans AM.** Nicotinic acid adenine dinucleotide phosphate mediates Ca^{2+} signals and contraction in arterial smooth muscle via a two-pool mechanism. *Circ Res* 91: 1168–1175, 2002.
5. **Bright NA, Gratian MJ, Luzio JP.** Endocytic delivery to lysosomes mediated by concurrent fusion and kissing events in living cells. *Curr Biol* 15: 360–365, 2005.
6. **Cancela JM, Churchill GC, Galione A.** Coordination of agonist-induced Ca^{2+}-signalling patterns by NAADP in pancreatic acinar cells. *Nature* 398: 74–76, 1999.
7. **Chen B, Wu Y, Mohler PJ, Anderson ME, Song LS.** Local control of Ca^{2+}-induced Ca^{2+} release in mouse sinoatrial node cells. *J Mol Cell Cardiol* 47: 706–715, 2009.
8. **Chowdhury I, Tharakan B, Bhat GK.** Current concepts in apoptosis: the physiological suicide program revisited. *Cell Mol Biol Lett* 11: 506–525, 2006.
9. **Christensen KA, Myers JT, Swanson JA.** pH-dependent regulation of lysosomal calcium in macrophages. *J Cell Sci* 115: 599–607, 2002.
10. **Churchill GC, Galione A.** Spatial control of Ca^{2+} signaling by nicotinic acid adenine dinucleotide phosphate diffusion and gradients. *J Biol Chem* 275: 38687–38692, 2000.
11. **Franzini-Armstrong C, Protasi F.** Ryanodine receptors of striated muscles: a complex channel capable of multiple interactions. *Physiol Rev* 77: 699–729, 1997.
12. **Kinnear NP, Boittin FX, Thomas JM, Galione A, Evans AM.** Lysosome-sarcoplasmic reticulum junctions. A trigger zone for calcium signaling by nicotinic acid adenine dinucleotide phosphate and endothelin-1. *J Biol Chem* 279: 54319–54326, 2004.
13. **Klee CB, Ren H, Wang X.** Regulation of the calmodulin-stimulated protein phosphatase, calcineurin. *J Biol Chem* 273: 13367–13370, 1998.
14. **Lee KH, Cho JH, Choi IS, Park HM, Lee MG, Choi BJ, Jang IS.** Pregnenolone sulfate enhances spontaneous glutamate release by inducing presynaptic Ca^{2+}-induced Ca^{2+} release. *Neuroscience* 171: 106–116, 2010.
15. **Lloyd-Evans E, Waller-Evans H, Peterneva K, Platt FM.** Endolysosomal calcium regulation and disease. *Biochem Soc Trans* 38: 1458–1464, 2010.
16. **Mukerjee N, McGinnis KM, Gnegy ME, Wang KK.** Caspase-mediated calcineurin activation contributes to IL-2 release during T cell activation. *Biochem Biophys Res Commun* 285: 1192–1199, 2001.
17. **Oshimi Y, Miyazaki S.** Fas antigen-mediated DNA fragmentation and apoptotic morphologic changes are regulated by elevated cytosolic Ca^{2+} level. *J Immunol* 154: 599–609, 1995.
18. **Patel S, Docampo R.** Acidic calcium stores open for business: expanding the potential for intracellular Ca^{2+} signaling. *Trends Cell Biol* 20: 277–286, 2010.
19. **Pryor PR, Mullock BM, Bright NA, Gray SR, Luzio JP.** The role of intraorganellar Ca(2+) in late endosome-lysosome heterotypic fusion and

in the reformation of lysosomes from hybrid organelles. *J Cell Biol* 149: 1053–1062, 2000.

20. **Rao RV, Castro-Obregon S, Frankowski H, Schuler M, Stoka V, del Rio G, Bredesen DE, Ellerby HM.** Coupling endoplasmic reticulum stress to the cell death program. An Apaf-1-independent intrinsic pathway. *J Biol Chem* 277: 21836–21842, 2002.
21. **Rathmell JC, Thompson CB.** Pathways of apoptosis in lymphocyte development, homeostasis, and disease. *Cell* 109, *Suppl*: S97–107, 2002.
22. **Ruas M, Rietdorf K, Arredouani A, Davis LC, Lloyd-Evans E, Koegel H, Funnell TM, Morgan AJ, Ward JA, Watanabe K, Cheng X, Churchill GC, Zhu MX, Platt FM, Wessel GM, Parrington J, Galione A.** Purified TPC isoforms form NAADP receptors with distinct roles for Ca(2+) signaling and endolysosomal trafficking. *Curr Biol* 20: 703–709, 2010.
23. **Santella L, Kyozuka K, Genazzani AA, De Riso L, Carafoli E.** Nicotinic acid adenine dinucleotide phosphate-induced Ca(2+) release. Interactions among distinct Ca(2+) mobilizing mechanisms in starfish oocytes. *J Biol Chem* 275: 8301–8306, 2000.
24. **Sasaki T, Kikuchi T, Yumoto N, Yoshimura N, Murachi T.** Comparative specificity and kinetic studies on porcine calpain I and calpain II with naturally occurring peptides and synthetic fluorogenic substrates. *J Biol Chem* 259: 12489–12494, 1984.
25. **Scoltock AB, Bortner CD, St J Bird G, Putney JW Jr, Cidlowski JA.** A selective requirement for elevated calcium in DNA degradation, but not early events in anti-Fas-induced apoptosis. *J Biol Chem* 275: 30586–30596, 2000.
26. **Shen D, Wang X, Li X, Zhang X, Yao Z, Dibble S, Dong XP, Yu T, Lieberman AP, Showalter HD, Xu H.** Lipid storage disorders block lysosomal trafficking by inhibiting a TRP channel and lysosomal calcium release. *Nat Commun* 3: 731, 2012.
27. **Shen D, Wang X, Xu H.** Pairing phosphoinositides with calcium ions in endolysosomal dynamics: phosphoinositides control the direction and specificity of membrane trafficking by regulating the activity of calcium channels in the endolysosomes. *Bioessays* 33: 448–457, 2011.
28. **Springer JE, Azbill RD, Nottingham SA, Kennedy SE.** Calcineurin-mediated BAD dephosphorylation activates the caspase-3 apoptotic cascade in traumatic spinal cord injury. *J Neurosci* 20: 7246–7251, 2000.
29. **Styrt B, Pollack CR, Klempner MS.** An abnormal calcium uptake pump in Chediak-Higashi neutrophil lysosomes. *J Leukoc Biol* 44: 130–135, 1988.
30. **Teng B, Ansari HR, Oldenburg PJ, Schnermann J, Mustafa SJ.** Isolation and characterization of coronary endothelial and smooth muscle cells from A_1 adenosine receptor-knockout mice. *Am J Physiol Heart Circ Physiol* 290: H1713–H1720, 2006.
31. **Wang X, Zhang X, Dong XP, Samie M, Li X, Cheng X, Goschka A, Shen D, Zhou Y, Harlow J, Zhu MX, Clapham DE, Ren D, Xu H.** TPC proteins are phosphoinositide- activated sodium-selective ion channels in endosomes and lysosomes. *Cell* 151: 372–383, 2012.
32. **Wozniak AL, Wang X, Stieren ES, Scarbrough SG, Elferink CJ, Boehning D.** Requirement of biphasic calcium release from the endoplasmic reticulum for Fas-mediated apoptosis. *J Cell Biol* 175: 709–714, 2006.
33. **Xu M, Zhang Y, Xia M, Li XX, Ritter JK, Zhang F, Li PL.** NAD(P)H oxidase-dependent intracellular and extracellular $O_2^{\cdot -}$ production in coronary arterial myocytes from CD38 knockout mice. *Free Radic Biol Med* 52: 357–365. 2012.
34. **Yamashima T.** Implication of cysteine proteases calpain, cathepsin and caspase in ischemic neuronal death of primates. *Prog Neurobiol* 62: 273–295, 2000.
35. **Yamashima T, Saido TC, Takita M, Miyazawa A, Yamano J, Miyakawa A, Nishijyo H, Yamashita J, Kawashima S, Ono T, Yoshioka T.** Transient brain ischaemia provokes Ca^{2+}, PIP2 and calpain responses prior to delayed neuronal death in monkeys. *Eur J Neurosci* 8: 1932–1944, 1996.
36. **Yamashima T, Tonchev AB, Tsukada T, Saido TC, Imajoh-Ohmi S, Momoi T, Kominami E.** Sustained calpain activation associated with lysosomal rupture executes necrosis of the postischemic CA1 neurons in primates. *Hippocampus* 13: 791–800, 2003.
37. **Zhang F, Jin S, Yi F, Li PL.** TRP-ML1 functions as a lysosomal NAADP-sensitive Ca^{2+} release channel in coronary arterial myocytes. *J Cell Mol Med* 13: 3174–3185, 2009.
38. **Zhang F, Xia M, Li PL.** Lysosome-dependent Ca^{2+} release response to Fas activation in coronary arterial myocytes through NAADP: evidence from CD38 gene knockouts. *Am J Physiol Cell Physiol* 298: C1209–C1216, 2010.
39. **Zhang F, Xu M, Han WQ, Li PL.** Reconstitution of lysosomal NAADP-TRP-ML1 signaling pathway and its function in TRP-$ML1^{-/-}$ cells. *Am J Physiol Cell Physiol* 301: C421–C430, 2011.
40. **Zhang G, Zhang F, Muh R, Yi F, Chalupsky K, Cai H, Li PL.** Autocrine/paracrine pattern of superoxide production through NAD(P)H oxidase in coronary arterial myocytes. *Am J Physiol Heart Circ Physiol* 292: H483–H495, 2007.
41. **Zinchuk V, Zinchuk O, Okada T.** Quantitative colocalization analysis of multicolor confocal immunofluorescence microscopy images: pushing pixels to explore biological phenomena. *Acta Histochem Cytochem* 40: 101–111, 2007.